


RESEARCH ARTICLE

High-performance triboelectric nanogenerator based on a double-spiral zigzag-origami structure for continuous sensing and signal transmission in marine environment

Yang Jiang^{1,2,3} | Pengfei Chen^{2,3} | Jiajia Han^{2,3} | Xi Liang^{2,4} |
Yutong Ming^{2,5} | Shijie Liu^{2,3} | Tao Jiang^{1,2,3}  | Zhong Lin Wang^{1,2}

¹Guangzhou Institute of Blue Energy, Guangzhou, China

²Beijing Key Laboratory of Micro-Nano Energy and Sensor, Center for High-Entropy Energy and Systems, Beijing Institute of Nanoenergy and Nanosystems, Chinese Academy of Sciences, Beijing, China

³School of Nanoscience and Engineering, University of Chinese Academy of Sciences, Beijing, China

⁴Beijing Key Laboratory for Nano-Photonics and Nano-Structure, Department of Physics, Capital Normal University, Beijing, China

⁵Key Laboratory of Urban Rail Transit Intelligent Operation and Maintenance Technology & Equipment of Zhejiang Province, The Institute of Precision Machinery and Smart Structure, College of Engineering, Zhejiang Normal University, Jinhua, Zhejiang, China

Correspondence

Tao Jiang and Zhong Lin Wang,
Guangzhou Institute of Blue Energy,
Knowledge City, Huangpu District,
Guangzhou 510555, China.
Email: jiangtao@binn.cas.cn and
zhong.wang@mse.gatech.edu

Funding information

National Key R & D Project from Minister of Science and Technology, Grant/Award Numbers: 2021YFA1201604, 2021YFA1201601; China National Postdoctoral Program for Innovative Talents, Grant/Award Number: BX20230357; Project supported by the Fundamental Research Funds for the Central Universities, Grant/Award Number: E3E46807X2; China Postdoctoral Science Foundation, Grant/Award Number: 2023M743445

Abstract

With the rapid evolution of emerging technologies like artificial intelligence, Internet of Things, big data, robotics, and novel materials, the landscape of global ocean science and technology is undergoing significant transformation. Ocean wave energy stands out as one of the most promising clean and renewable energy sources. Triboelectric nanogenerators (TENGs) represent a cutting-edge technology for harnessing such random and ultra-low frequency energy toward blue energy. A high-performance TENG incorporating a double-spiral zigzag-origami structure is engineered to achieve continuous sensing and signal transmission in marine environment. Integrating the double-spiral origami into the TENG system enables efficient energy harvesting from the ocean waves by converting low-frequency wave vibrations into high-frequency motions. Under the water wave triggering of 0.8 Hz, the TENG generates a maximum peak power density of 55.4 W m^{-3} , and a TENG array with six units can generate an output current of $375.2 \mu\text{A}$ (density of 468.8 mA m^{-3}). This power-managed TENG array effectively powers a wireless water quality detector and transmits signals without an external power supply. The findings contribute to the development of sustainable and renewable energy technologies for oceanic applications and open new

Yang Jiang and Pengfei Chen contributed equally to this study.

This is an open access article under the terms of the [Creative Commons Attribution](https://creativecommons.org/licenses/by/4.0/) License, which permits use, distribution and reproduction in any medium, provided the original work is properly cited.

© 2024 The Author(s). *Interdisciplinary Materials* published by Wuhan University of Technology and John Wiley & Sons Australia, Ltd.

pathways for designing advanced materials and structures in the field of energy harvesting.

KEYWORDS

blue energy harvesting, double-spiral zigzag-origami structure, ocean sensor, triboelectric nanogenerator, wireless water quality monitoring

1 | INTRODUCTION

Water quality monitoring plays a vital role in safeguarding entire aquatic environments, controlling pollution, and sustaining the health of water ecosystems.^[1–5] Traditional methods for nearshore marine water quality monitoring rely on manual sampling and monitoring.^[6] However, these methods are hindered by complex weather conditions and sea state environments, necessitating a significant workforce and specialized equipment, resulting in low efficiency, poor real-time performance, and limited monitoring coverage. Intelligent ocean sensors have emerged with the progression of the Internet of Things (IoTs) technology and ocean engineering.^[7–10] These sensors encompass buoy-based detection, satellite detection, aerial detection, and unmanned surface vessel detection, furnishing data support for studying marine water quality environments and hydrodynamic characteristics.^[11–13] Marine environmental monitoring entails long durations and challenges in recycling and replacing batteries.^[14–16] Therefore, there is a pressing need to develop intelligent sensors with low power consumption for sustainable monitoring.^[17–20]

The quest for a self-sustaining power generation system utilizing renewable energy sources has garnered significant interests and demands. Ocean wave energy represents one of the cleanest and most renewable energy sources, meriting widespread applications.^[21,22] It offers the advantages of abundant reserves and minimal dependence on surrounding environmental conditions. However, this energy source remains untapped mainly due to the resource constraints and lack of effective energy harvesting technologies. Typically, ocean waves exhibit low frequencies, rendering conventional electromagnetic generators (EMGs) unsuitable due to their inefficiency.^[23,24] Considering the significant challenges faced by EMGs, including high costs, susceptibility to corrosion, and low efficiency at low frequencies, the development of a cost-effective, lightweight, and efficient technology holds crucial practical significance for harnessing water wave energy.

Triboelectric nanogenerator (TENG), invented in 2012, has garnered significant attention for its outstanding performance, indicating its potential to offer

sustainable and clean energy for portable electronic devices and various sensing technologies by converting environmental mechanical energy into electrical energy.^[25–28] The TENG technology, adopting the mechanism of Maxwell's displacement current, has been employed to harness energy from diverse sources, boasting high power density, efficiency, and cost-effectiveness. Relative to the EMG, the TENG demonstrates superior performance at low frequencies, making it ideal for ultra-low-frequency wave energy harvesting.^[29–33] Numerous TENG prototypes have been developed to capture water wave energy efficiently, showcasing the potential of large-scale blue energy harvesting. However, many existing TENG devices operate close to the triggering frequency of water waves, resulting in suboptimal performance due to the low frequency of water waves. There is still a long way to realize commercialization at this stage, and the main problem is that the performance of TENGs under water waves needs to be further enhanced to meet commercial standards.^[34–36] Various strategies, including material selection based on electro-negativity differences, material functionalization, micro-structural engineering to enhance surface contact area, and structural design, have been proposed to improve the output performance. The material surface modification by micromachining or chemical methods to construct micro/nano structures plays a pivotal role in influencing the electrification properties of materials, thereby elevating the output performance of TENGs.^[37–41] Furthermore, reasonable structural design can optimize the interaction between the TENG devices and water waves, enhancing the working effect of TENGs. Our previous research has introduced an origami structure to improve performance by amplifying the operating frequency through a zigzag design. While this zigzag TENG design offers robustness, durability, and flexibility, further enhancements are necessary to realize practical applications of blue energy harvesting. Deepening our understanding of water wave response mechanisms is crucial for refining TENG performance and advancing blue energy utilization.

Herein, a high-performance TENG is presented with a double-spiral zigzag-origami structure (D-Z-shaped TENG) for harvesting water wave energy and

integrated with a set of power management circuits (PMCs) to manage the output energy. Under the water wave excitation at 0.8 Hz, the peak power density reaches 55.4 W m^{-3} and the average power density reaches 2.1 W m^{-3} at the matched resistance. A TENG array consisting of six TENG units can generate an output current of $375.2 \mu\text{A}$ and a current density of 468.8 mA m^{-3} . Finally, this power-managed TENG array can effectively power a wireless water quality detector and transmit signals without an external power supply, indicating the extensive applications of TENGs toward blue energy.

2 | RESULTS AND DISCUSSION

2.1 | Application scenario and structure of the D-Z-shaped TENG

Underwater sensor networks play a crucial role in complete military and civilian applications such as ocean monitoring and resource exploration, which are the first choices for countries when developing and utilizing marine resources. As shown in Figure 1A, the TENG employs a D-Z-shaped structure, meaning that the networks can harvest energy from water, collect marine

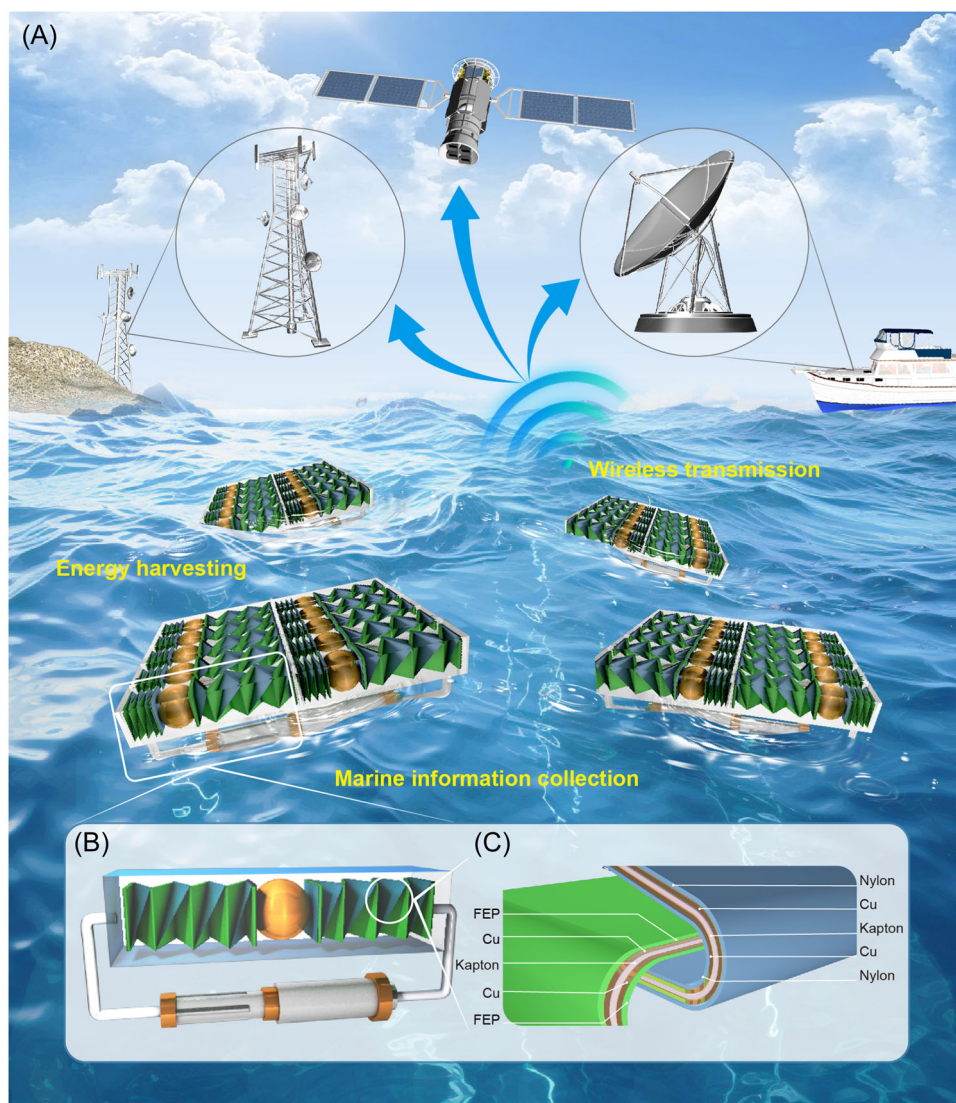


FIGURE 1 Application scenario and structure of the D-Z-shaped TENG. (A) Concept proposed for applying the D-Z-shaped TENG in the intelligent ocean. (B) Illustration of the structure for D-Z-shaped TENG, comprising two strips. The TENG is constructed with a double-spiral zigzag-origami structure, essentially forming a spring. It leverages the contact and separation of the origami layers due to the fluctuation of the waves to harness wave energy for powering ocean sensors. (C) Schematic diagram of the local part of D-Z-shaped TENG: one strip is comprised of the FEP layer, Cu layer, Kapton layer, Cu layer, and FEP layer. The other strip is composed of the nylon layer, Cu layer, Kapton layer, Cu layer, and nylon layer. TENG, triboelectric nanogenerator.

information, and transmit the sensing signals in water. As shown in Figure 1B, the structure for the D-Z-shaped TENG comprises two strips. The double-spiral zigzag-origami structure in the TENG essentially forms a spring. It leverages the contact and separation of the origami layers due to the fluctuation of the waves to harness wave energy for powering ocean sensors. A detailed schematic diagram of the D-Z-shaped TENG is shown in Figure 1C. One strip is comprised of the fluorinated ethylene propylene (FEP) layer, copper (Cu) layer, Kapton layer, Cu layer, and FEP layer of 10 μm thick and 60 cm long. The other strip comprises the nylon layer, Cu layer, Kapton layer, Cu layer, and nylon layer. Square copper electrodes of 3×3 cm were printed on both the front and back of these strips to form the electrodes of the TENG. An FEP film was attached to both sides of one strip and subjected to high-voltage polarization to function as the negative electrode. Conversely, a nylon film was affixed to both sides of the other strip, serving as the positive electrode. The two equal-length strips were then folded and glued together in a simple crease pattern. In this configuration, the strips were alternately staggered and folded into an origami structure, creating a spring-like form. This design eliminates the need for springs, steel shafts, and other space-consuming components, thereby freeing up significant space for more extensive multilayered TENGs. Moreover, the differences between the TENGs based on the D-Z-shaped and Z-shaped structures are compared in Supporting Information: Figure S1–S4. This shows that the D-Z-shaped structure can be more significantly compressed due to the unique spring structure of the appropriate stiffness.

2.2 | Electrical measurements of the D-Z-shaped TENGs

Power generation in a TENG typically occurs through contact electrification and electrostatic induction phenomena. When triboelectric materials with different electronegativities come into contact, surface charges are generated at their interface due to the charging effect. Upon separation of these materials by an external force, induced charges are created on the back conductive electrodes through electrostatic induction. These charges are transferred across an external load until potential equilibrium is reached. The schematic working principle is illustrated in Supporting Information: Figure S5. The origami length of the TENG device is an essential parameter for the output performance. The electrical outputs of the D-Z-shaped TENGs with different lengths of origami strips under different frequencies are shown in Figure 2A–C. A linear motor was utilized to drive the

D-Z-shaped TENGs to perform linear reciprocating motion for controlling the frequency to reduce variables. When adjusting the spring origami length from 30 cm to 60 cm and to 90 cm, the voltage of the D-Z-shaped TENG at 30 cm is roughly the maximum for each frequency. Because at 30 cm, the TENG can contact and separate more fully, especially under 1.25, 1.5, and 1.75 Hz. The voltage decrease with increasing the spring origami length is ascribed to the insufficient contact separation and the next little increase is because of the increased contact area (Figure 2A). On the other hand, under different frequencies, the current of the D-Z-shaped TENGs first increases and then decreases as the spring origami length increases, as shown in Figure 2B. The current at 60 cm reaches the maximum, which is slightly higher than that at 30 or 90 cm. Moreover, the trend of transferred charge is similar to the current, but the charge at 60 cm is much larger than that at 30 cm, as shown in Figure 2C. As a result, the origami length of 60 cm was chosen for making the D-Z-shaped TENGs.

To study the other influences of the electrical outputs, the D-Z-shaped TENGs with an origami length of 60 cm under different frequencies were measured by the dynamic torque measurement system which imitates the swaying of water waves (Figure 2D–F). The output voltage has nearly no change with the frequency ranging from 0.25 to 1.75 Hz as presented in Figure 2D. Figure 2E shows that the output current first increases and then decreases slightly with increasing frequency. Moreover, the transferred charge of the TENG changes similarly to the output current, as shown in Figure 2F. In addition, different strip connection methods that may have an impact on the TENG unit outputs have been investigated. Figure 2G shows that the single strip achieves the maximum output voltage under different frequencies compared to the series and parallel connections. This result can be attributed to the ample space for the single strip to complete contact and separation. Figure 2H indicates the output current of the TENG with the origami length of 60 cm under different frequencies can get the highest for the series connection of the two strips among the three strip connection methods. What's more, the D-Z-shaped TENG also achieves the highest transferred charge in the series connection, as shown in Figure 2I.

Subsequently, the D-Z-shaped TENG's output voltage, output current, and transferred charge were measured in real water waves with different frequencies under the wave height of 14 cm, as shown in Figure 3A–C. As the wave frequency varies from 0.4 to 1.2 Hz, the TENG outputs first increase and then decrease, leading to the maximum values of 387.3 V, 58.6 μA , and 1.2 μC at the frequency of 0.8 Hz. The initial boost in output performance with the frequency is due to the accelerated

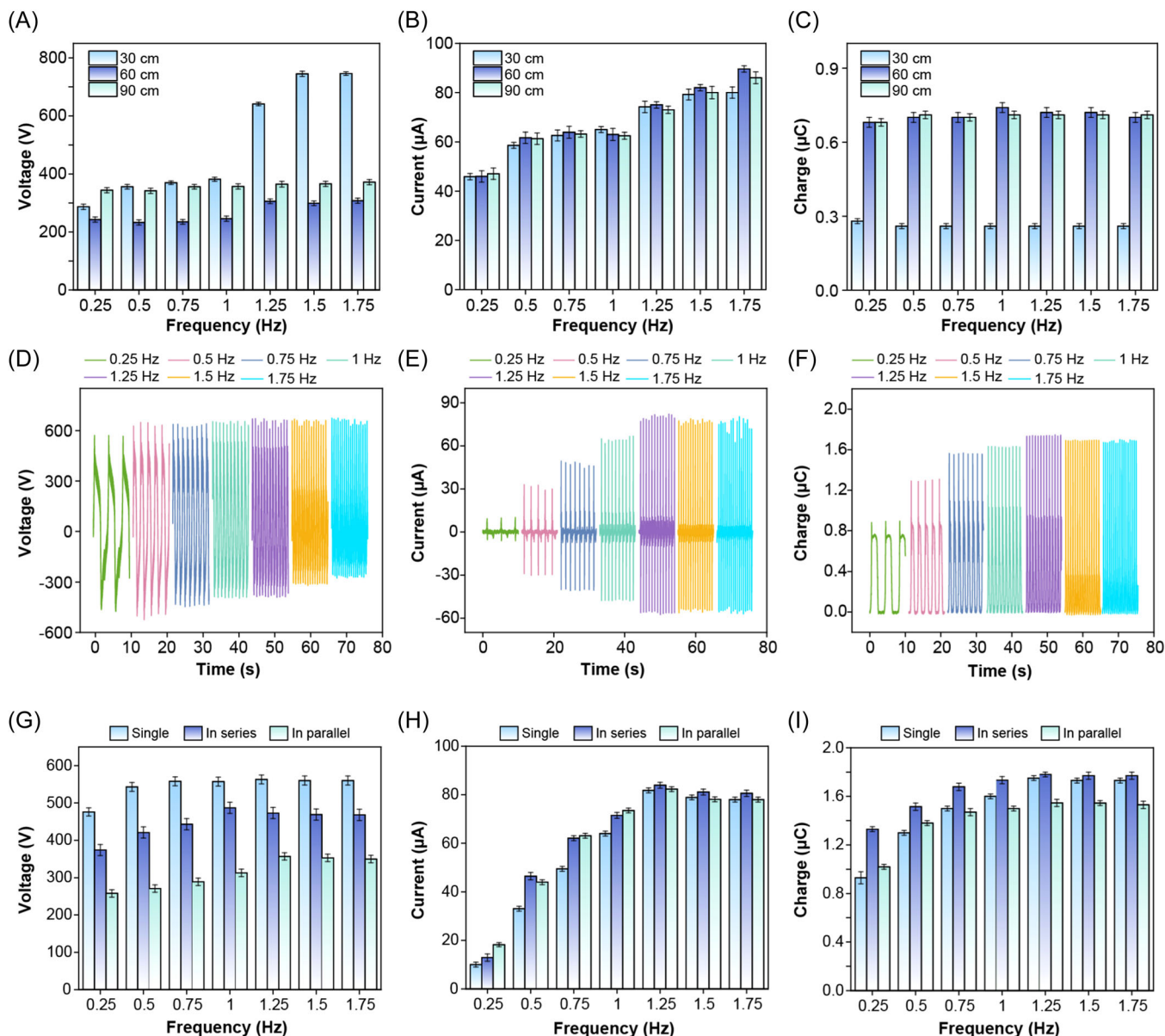


FIGURE 2 Electrical measurements of the D-Z-shaped TENGs. (A) Output voltage, (B) output current, and (C) transferred charge of the D-Z-shaped TENGs with different lengths of origami strips under different frequencies. (D–F) Typical voltage, current, and charge profiles of the D-Z-shaped TENGs with the origami length of 60 cm under different frequencies. (G) Output voltage, (H) output current, and (I) transferred charge of the D-Z-shaped TENGs with the origami length of 60 cm for different strip connection methods under different frequencies. TENGs, triboelectric nanogenerators.

velocity of the copper ball, thereby intensifying the pressure exerted on the D-Z-shaped TENG. However, when the wave frequency is higher than 0.8 Hz, the copper ball can quickly oscillate unstably, and the shorter vibration period causes the insufficient pressing on the multilayered TENGs. The optimal frequency is primarily determined by the entire structure, including the copper ball and origami within the device. Additionally, the impact of wave height on the TENG outputs was investigated, as shown in Figure 3D–F. The output performance of the D-Z-shaped TENG increases with increasing

the wave height at the optimum frequency of 0.8 Hz. In essence, larger wave heights enhance the TENG's operation, whereas slight water waves with small wave heights fail to fully activate the TENG due to the device weight, resulting in decreased output performance. Figure 3G illustrates the typical working states of D-Z-shaped TENG in water. At the longest origami length ($L = 60$ mm), the D-Z-shaped TENG achieves the maximum peak power density of 55.4 W m^{-3} under the water wave frequency of 0.8 Hz (Figure 3H). Besides the magnitude of the output peaks, the output frequency is also

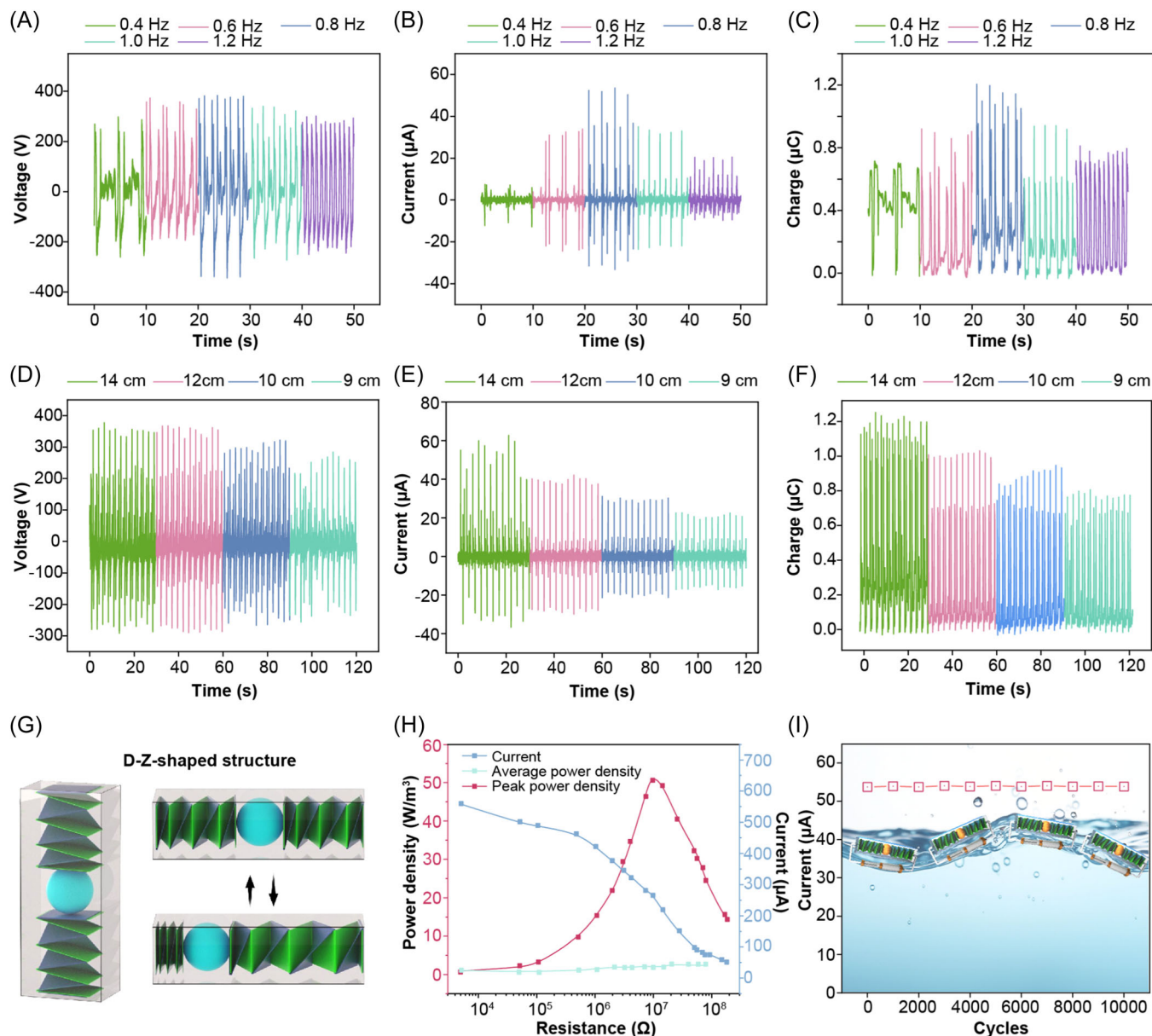


FIGURE 3 Influences of water wave frequencies and heights on the electrical outputs of the D-Z-shaped TENG. (A–C) Electrical output performance of the D-Z-shaped TENG at different wave frequencies under wave height of 14 cm, including output voltage, output current, and transferred charge. (D–F) Waveforms of the electrical outputs of the D-Z-shaped TENG at various wave heights, including output voltage, output current, and transferred charge. (G) Schematic diagram illustrating the working states of the D-Z-shaped TENG. (H) Peak current, peak power density, and average power density of the D-Z-shaped TENG with respect to the loading resistance under the wave frequency of 0.8 Hz. (I) Variation of the current under continuous measurements for 10 000 cycles. TENG, triboelectric nanogenerator.

enhanced by the origami spring. The results show that the D-Z-shaped origami structure can improve the contact force between the triboelectric materials in each TENG unit and strengthen the reciprocation of the swing component. Device stability is also essential for energy harvesting, and Figure 3I shows the excellent stability of the D-Z-shaped TENG under continuous measurements for 10 000 cycles in water waves.

The arrangement manner of the units in a TENG array may influence the electric outputs of the array

because of the water waves' irregular movements. In detail, Figure 4A,B demonstrates the D-Z-shaped TENG arrays consisting of six units in horizontal and vertical configurations. Figure 4C compares the average power densities of the horizontal array and vertical array using the D-Z-shaped TENGs under the wave frequency of 0.8 Hz. It indicates that the power densities of the two arrays of the D-Z-shaped TENGs reach the maximum values at 10 M Ω . What's more, the result also shows that the horizontal array of D-Z-shaped TENGs can generate a

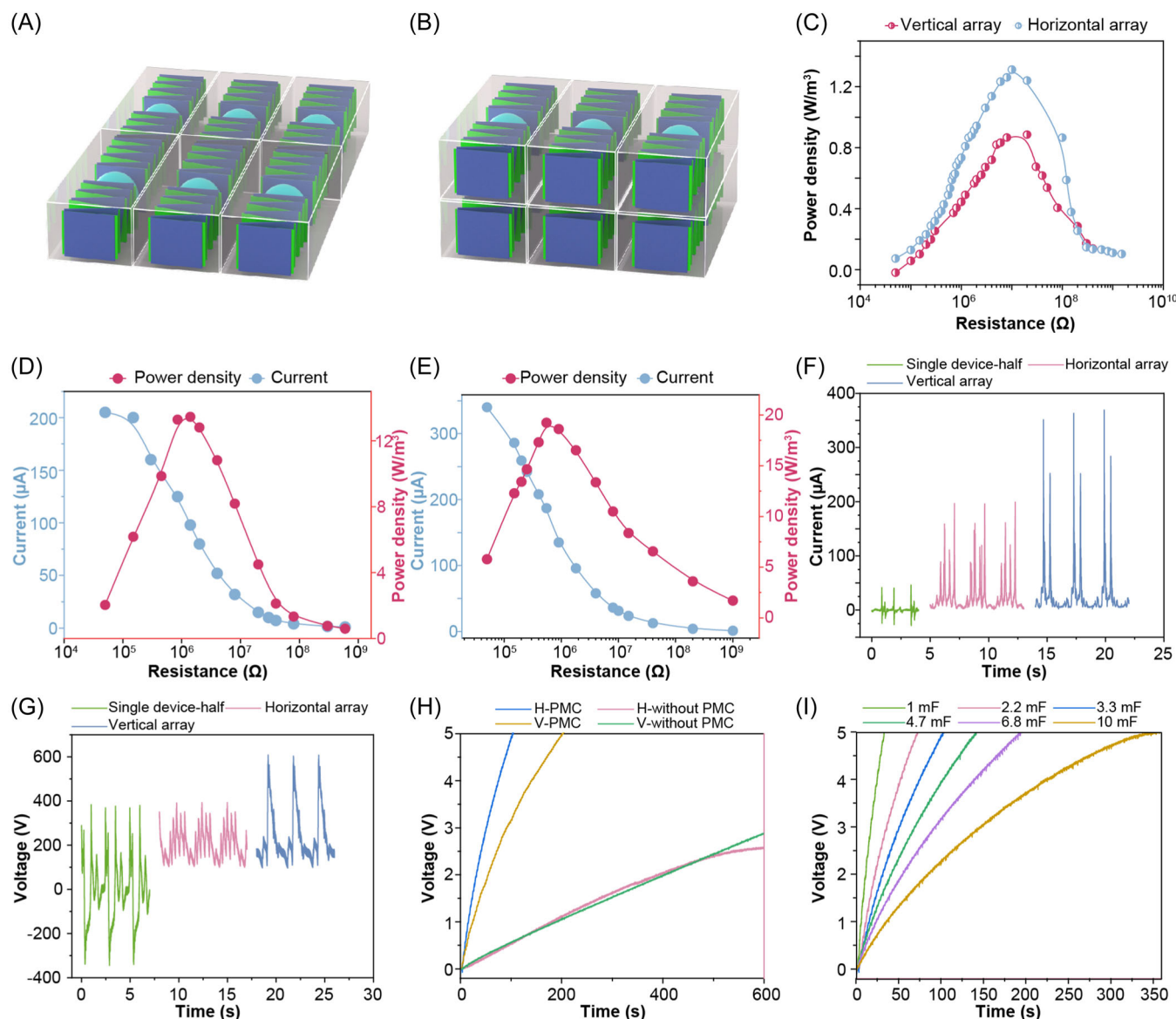


FIGURE 4 Electrical output performance of the D-Z-shaped TENG arrays. (A, B) Demonstrations of the D-Z-shaped TENG arrays in horizontal and vertical configurations. (C) Comparison of average power densities of the horizontal and vertical arrays using the D-Z-shaped TENGs under the water frequency of 0.8 Hz. (D) Peak current and peak power density of the horizontal TENG array with respect to the loading resistance under the wave frequency of 0.8 Hz. (E) Peak current and peak power density of the vertical TENG array. (F, G) Comparison of output performance among the single D-Z-shaped TENG, horizontal array, and vertical array under the water frequency of 0.8 Hz, including the output current and voltage. (H) Comparison of charging voltage on 150 and 200 μF capacitors with or without the PMC for the horizontal array and vertical array. (I) Charging voltage on various capacitors for the horizontal D-Z-shaped TENG array. TENG, triboelectric nanogenerator.

higher average power density than the vertical array. Figure 4D presents the current and peak power density of the horizontal TENG array with respect to the load resistance under the water frequency of 0.8 Hz. It is apparent that the peak power density first increases and then decreases, reaching the maximum value of 15.8 W m^{-2} . As shown in Figure 4E, the peak power density of the vertical array arrives at the maximum value of 19.2 W m^{-2} at the frequency of 0.8 Hz and the

matched resistance of $1.0 \text{ M}\Omega$. Moreover, Figure 4F,G compare the output performance of the single D-Z-shaped TENG, horizontal array, and vertical array under the water frequency of 0.8 Hz, including the output current and voltage. The results present that the vertical array has a maximum current of $375.2 \mu\text{A}$ and voltage of 615.9 V . Figure 4H is the comparison graphs of charging 150 and $200 \mu\text{F}$ capacitors directly or through integration with the PMCs, exhibiting five times improvement in the

charging speed. Furthermore, the comparison of charging voltage to a 3.3 mF capacitor between direct charging and managed charging are shown for the horizontal array (Supporting Information: Figure S6) and vertical array (Supporting Information: Figure S7). Figure 4I and Supporting Information: Figure S7 show the charging voltage on various capacitances from 1 to 10 mF for the D-Z-shaped TENGs with the two different array manners. The curves depict that the charging voltage rapidly increases and then gradually stabilizes, which is associated with the capacitance and gets higher for smaller capacitance. The ability of the TENG array to continuously power devices without the need for an external power source which highlights its potential to revolutionize blue energy harvesting and provide a powerful renewable solution for promoting marine technology. This breakthrough paves the way for further innovations in materials science and structural engineering, which are expected to increase the efficiency and application range of energy harvesting technologies in marine environments and beyond.

2.3 | Application demonstrations of the D-Z-shaped TENGs

Converting the dispersed mechanical energy in the environment into an effective and stable energy is the strongest evidence of energy harvesting capability for TENG devices. Numerous previous works have demonstrated that the TENG devices are able to light up liquid crystal display (LCD) screens of digital thermometers, but they only complete one-time indication work, due to limited energy harvesting speed and imperfect power management circuit. Therefore, the completion of continuous energy supply and autonomous information transmission has always been the ultimate goal of self-powered systems. Aiming at this goal, we designed a set of PMCs that integrate efficient energy harvesting and on-demand energy supply, as shown in Figure 5A,B. Figure 5A shows a system flow chart of D-Z-shaped TENG for harvesting mechanical energy and providing stable energy for the wireless sensing unit. In this situation, many commercial sensors can be driven and achieve a fully self-powered IoTs sensor node that integrates energy harvesting, data processing, and wireless signal transmission. First, the D-Z-shaped TENG converts the water wave energy into electrical energy that will be stored in the buffer capacitor C_{in} through the rectifier circuit. The PMC then completes the voltage reduction and current elevation and realizes efficient energy storage in the capacitor C_{out} . This is the main function of the M_1 module. After that, the sufficient

energy accumulated in C_{out} that meets the load demand is effectively supplied to the load for a certain period under the control of M_2 module to complete the function of information collection and signal transmission. When there is insufficient energy on the C_{out} , the M_2 module will automatically turn off the energy supply to the load and restart the energy accumulation.

Figure 5C shows the voltage curves across the C_{out} of 1 mF (red curve) and load (blue curve) during the above-mentioned automatic energy supply period. Under the excitation of water waves, the digital thermo-hygrometer intermittently energizes the capacitor C_{out} for three times and transmits real-time signals to the mobile phone via Bluetooth. The enlarged figure is shown in Figure 5D. First, the D-Z-shaped TENG charges the capacitor to power the thermo-hygrometer, and the thermo-hygrometer is activated but without data transmission. After a few seconds, the mobile phone's Bluetooth is turned on. At that period, the thermo-hygrometer collects the temperature and humidity data and transmits them to the mobile phone. The result shows that the digital thermo-hygrometer can constantly work and transmit data after 100 s of powering by the D-Z-shaped TENG, demonstrating its excellent power supply capability, as shown in Supporting Information: Video S1.

Besides, as we all know, the power consumption of the commercial water quality detector (CWQD) is greater than that of the digital thermo-hygrometer, which makes it challenging to achieve a constant power supply. Therefore, an 8 mAH lithium-ion battery was used as an energy storage unit instead of the C_{out} to meet the requirement of such large energy consumption load. Figure 5E demonstrates the voltage on the lithium-ion battery and the CWQD. First, the voltage of the lithium-ion battery charged by the TENG increases slowly, at which time the voltage at both ends of the CWQD is 0, that is, the M_2 is in the off state. After charging for 2000 s, when the voltage reaches 3.3 V, the power switch is turned on automatically. Then, the CWQD works and tests the water quality information, such as the total dissolved solids (TDS) and pH values. Similarly, the CWQD transmits the data to the mobile phone when the Bluetooth is turned on. Supporting Information: Video S2 shows the process of powering the CWQD again by the D-Z-shaped TENG and transmitting data after 1000 s. This fully demonstrates the powerful energy harvesting capability of our TENG device for charging lithium-ion batteries, and also illustrates the significant advantage of our self-designed PMCs. However, the limitation of Bluetooth transmission distance severely hinders the applications of TENGs in self-powered marine sensor nodes. Therefore, based on the Zigbee protocol, we

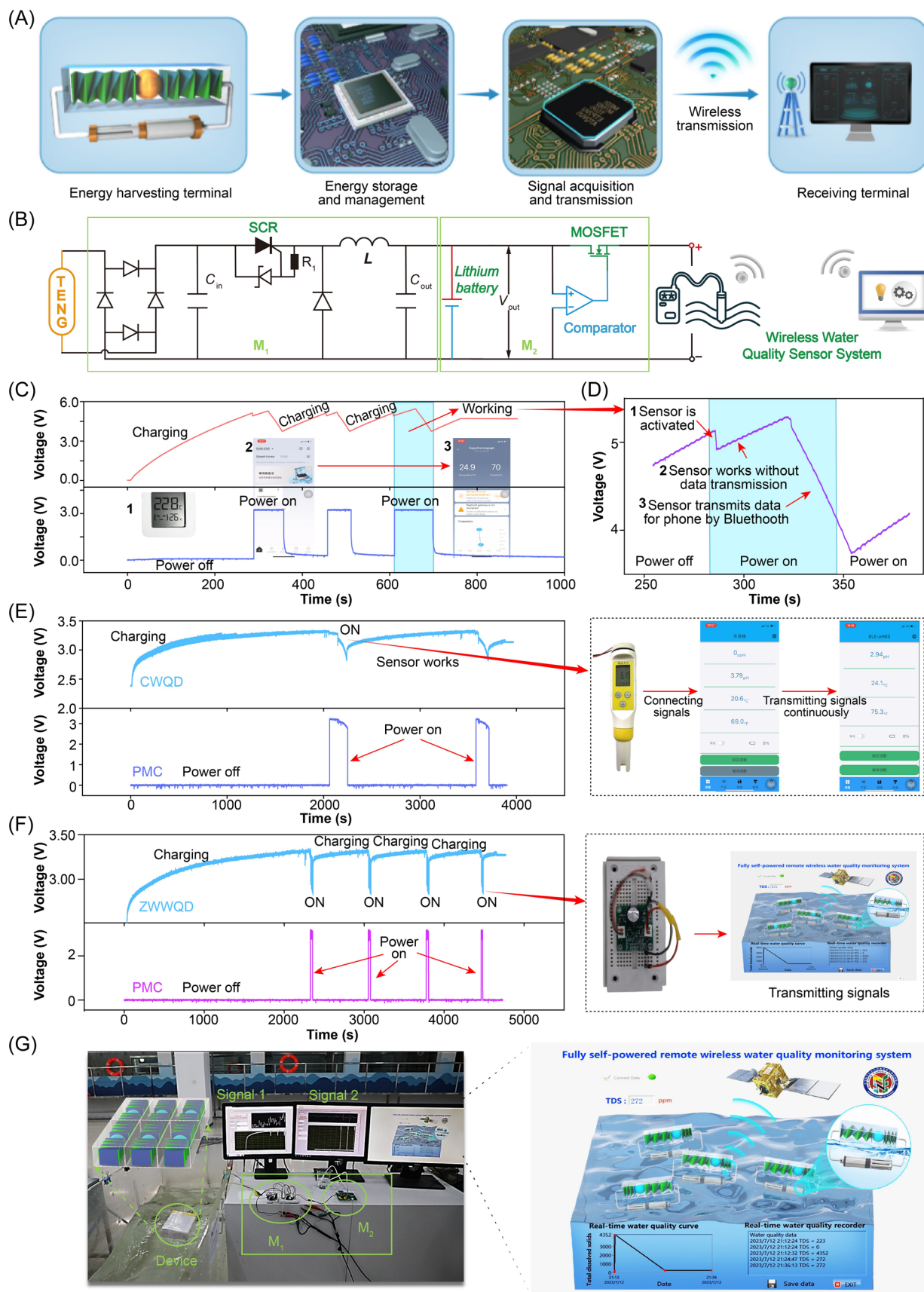


FIGURE 5 (See caption on next page).

further designed the wireless water quality detector (ZWWQD) module. Thanks to the low power consumption of data transmitting by Zigbee wireless transmission protocol, the power consumptions of our wireless water quality detector is 33.6 mW. This module can realize the function of automatic signal transmission after power on and achieve a longer distance signal transmission (about 100 m). At the same time, we also designed the corresponding remote information display client to display the received data intuitively. Figure 5F shows the voltage curves at both ends of the battery and the ZWWQD during the energy harvesting process. Figure 5G is the physical diagram of the experiment setup and the display interface of the client during the experiments. We can clearly see that the ZWWQD was successfully powered for four times and transmitted the signals to the remote client. What's more, Supporting Information: Video S3 shows the experiment of wireless transmission via the D-Z-shaped TENG in natural water. The TENG successfully powers the ZWWQD, and when the voltage achieves the 3.2 V, the Bluetooth is turned on to transmit data. That means the TENG can continuously power sensors in the sea without an external power source. It will significantly promote the development of TENG as a power source for fully self-powered systems. It is a milestone for the TENG to successfully charge lithium-ion batteries under natural water waves and continue powering water quality detectors and sending signals, laying a solid foundation for its practical applications.

3 | CONCLUSION

This paper introduces a high-performance TENG based on a double-spiral zigzag-origami structure for harvesting water wave energy and integrates it with a set of PMCs to manage the output energy. Under the water wave excitation at 0.8 Hz, the peak power density reached 55.4 W m^{-3} , and the average power density reached 2.1 W m^{-3} at the matched resistance. A TENG array consisting of six TENG units can generate an output current of $375.2 \mu\text{A}$, and a current density of 468.8 mA m^{-3} . The development of TENGs utilizing the novel

double-spiral zigzag-origami structure marks a significant advancement in the field of sustainable ocean energy technologies. This innovative TENG design optimizes energy capturing and supports continuous sensing and data transmission capabilities essential for modern oceanography by effectively harnessing the irregular, low-frequency wave motion energy prevalent in marine environments. The demonstrated ability of a TENG array to power devices such as water quality detectors continuously and transmit data for mobile phone without external electricity underscores its potential to revolutionize blue energy collection, offering a robust, renewable solution for promoting ocean technologies. The existing photovoltaic technology can produce higher output power, but the effective output energy is limited due to the shorter sunshine time and working time. At present stage, the TENGs are expected to hybridize with the solar panels to establish a comprehensive composite platform for capturing multiple kinds of energy sources. This breakthrough paves the way for further innovations in materials science and structural engineering, which is promising to enhance the efficiency and application scope of energy harvesting technologies in marine settings and beyond.

4 | EXPERIMENTAL SECTION

4.1 | Fabrication of the D-Z-shaped TENG device

First, two strips of Kapton film, each $10 \mu\text{m}$ thick and 60 cm long, were used as the substrate. Square copper electrodes of $3 \times 3 \text{ cm}$ were printed on both the front and back of these strips to form the electrodes of the TENG. An FEP film was attached to both sides of one strip and subjected to high-voltage polarization to function as the negative electrode. Conversely, a nylon film was affixed to both sides of the other strip, serving as the positive electrode. The two equal-length strips were then folded and glued together in a simple crease pattern. In this configuration, the strips were alternately staggered and folded into an origami structure, creating a spring-like

FIGURE 5 Application demonstrations of the D-Z-shaped TENG for water wave energy harvesting. (A) A flow chart using the D-Z-shaped TENG to drive the sensing module and transmit signals wirelessly. (B) Circuit diagram of the output management circuit and ultra-low power discharge management circuit to power electronic devices. (C) Charging and discharging process of the C_{out} to power the thermo-hygrometer by the D-Z-shaped TENG integrated with the two PMC modules. (D) Enlarged charging voltage curve on the C_{out} when the thermo-hygrometer works. (E) Charging and discharging process of the C_{out} to power the CWQD by the power-managed D-Z-shaped TENG. (F) Voltage curve on the 8 mAh lithium-ion battery during its charging and discharging process and voltage on the ZWWQD by the power-managed D-Z-shaped TENG in the water waves. (G) Photograph of the simulation test for realizing wireless transmission via the D-Z-shaped TENG in the water waves, and the enlarged figure is the computer interface. CWQD, commercial water quality detector; TENG, triboelectric nanogenerator.

form. This design eliminates the need for springs, steel shafts, and other space-consuming components, thereby freeing up significant space for TENGs.

The D-Z-shaped TENGs used tile cement for sealing and waterproofing for the water wave energy harvesting. Part A and part B of tile cement were mixed in the volume ratio of 1:1 and stirred until well distributed. Finally, the edge of the acrylic shells was sealed by the mixture. The conducting wires were connected with the rectifiers through the holes of the acrylic shell and then connected in parallel in each TENG unit. The six TENGs were respectively connected to a full-bridge rectifier and then connected in parallel.

4.2 | Electric measurements of the TENG device

The primary electric outputs of the D-Z-shaped TENGs and TENG array device were measured under the water waves generated by using a series of wave pumps (rw-20 JEPOWER TECHNOLOGY Inc.) controlled by a function generator (AFG3011C Tektronix Inc.). The output current, transferred charges, and output voltage of the TENGs were measured by the Keithley 6514 System Electrometer.

ACKNOWLEDGMENTS

Y. J. and P. C. contributed equally to this work. The authors thank the National Key R & D Project from Minister of Science and Technology (2021YFA1201604, 2021YFA1201601), the China National Postdoctoral Program for Innovative Talents (BX20230357), Project supported by the Fundamental Research Funds for the Central Universities (E3E46807X2), and the China Postdoctoral Science Foundation (2023M743445).

CONFLICT OF INTEREST STATEMENT

The authors declare no conflict of interest.

DATA AVAILABILITY STATEMENT

The data that supports the findings of this study are available in the Supporting Information of this article.

ORCID

Tao Jiang  <http://orcid.org/0000-0001-7941-7703>

REFERENCES

- [1] Alshami A, Ali E, Elsayed M, Eltoukhy AEE, Zayed T. IoT innovations in sustainable water and wastewater management and water quality monitoring: a comprehensive review of advancements, implications, and future directions. *IEEE Access*. 2024;12:58427-58453.
- [2] Behmel S, Damour M, Ludwig R, Rodriguez MJ. Water quality monitoring strategies—a review and future perspectives. *Sci Total Environ*. 2016;571:1312-1329.
- [3] Chen Y, Han D. Water quality monitoring in smart city: a pilot project. *Autom Constr*. 2018;89:307-316.
- [4] Li Y, Fu Y, Lang Z, Cai F. A high-frequency and real-time ground remote sensing system for obtaining water quality based on a micro hyper-spectrometer. *Sensors*. 2024;24(6):1833.
- [5] Thombare BR, Daware KD, Khupse N, et al. Smart nanocomposites: harnessing magnetically recoverable MWCNT-CF for efficient organic dyes reduction in water quality monitoring applications. *AIP Adv*. 2024;14(2):025140.
- [6] Domingo MC. An overview of the internet of underwater things. *J Netw Comput Appl*. 2012;35(6):1879-1890.
- [7] Otto A, Tilk C. Intelligent design of sensor networks for data-driven sensor maintenance at railways. *Omega*. 2024;127:103094.
- [8] Tsabaris C, Bozzano R. Application of coastal/ocean sensors and systems. *J Mar Sci Eng*. 2024;12(1):91.
- [9] Zou Y, Sun M, Li S, et al. Advances in self-powered triboelectric sensor toward marine IoT. *Nano Energy*. 2024;122:109316.
- [10] Li H, Liu W, Sun G, et al. Concept of spaceborne ocean microwave dual-function integrated sensor for wind and wave measurement. *Remote Sens*. 2024;16(8):1472.
- [11] Briciu-Burghina C, Power S, Delgado A, Regan F. Sensors for coastal and ocean monitoring. *Annu Rev Anal Chem*. 2023;16(1):451-469.
- [12] Chen WH, Dillon WDN, Armstrong EA, Moratti SC, McGraw CM. Self-referencing optical fiber pH sensor for marine microenvironments. *Talanta*. 2021;225:121969.
- [13] Gu Y, Cui S, Ke C, Zhou K, Liu D. All-digital timing recovery for free space optical communication signals with a large dynamic range and low OSNR. *IEEE Photonics J*. 2019;11(6):1-11.
- [14] Liu T, Zhang L, Cheng B, Yu J. Hollow carbon spheres and their hybrid nanomaterials in electrochemical energy storage. *Adv Energy Mater*. 2019;9(17):1803900.
- [15] Lucas A, Pintel R, Alford M. Ocean wave energy for long endurance, broad bandwidth ocean monitoring. *Oceanography*. 2017;30(2):126-127.
- [16] Qiu T, Zhao Z, Zhang T, Chen C, Chen CLP. Underwater internet of things in smart ocean: system architecture and open issues. *IEEE Trans Industr Inform*. 2020;16(7):4297-4307.
- [17] Raj A, Steingart D. Review-power sources for the internet of things. *J Electrochem Soc*. 2018;165(8):B3130-B3136.
- [18] Shi B, Li Z, Fan Y. Implantable energy-harvesting devices. *Adv Mater*. 2018;30(44):e1801511.
- [19] Wang X, Shang J, Luo Z, Tang L, Zhang X, Li J. Reviews of power systems and environmental energy conversion for unmanned underwater vehicles. *Renew Sustain Energy Rev*. 2012;16(4):1958-1970.
- [20] Yang J, Wen J, Wang Y, Jiang B, Wang H, Song H. Fog-based marine environmental information monitoring toward ocean of things. *IEEE Internet Things J*. 2020;7(5):4238-4247.
- [21] Awan KM, Shah PA, Iqbal K, Gillani S, Ahmad W, Nam Y. Underwater wireless sensor networks: a review of recent issues and challenges. *Wirel Commun Mob Comput*. 2019;2019:1-20.
- [22] Heath TV. A review of oscillating water columns. *Philos Trans R Soc, A*. 2012;370(1959):235-245.

- [23] Wu Z, Guo H, Ding W, Wang YC, Zhang L, Wang ZL. A hybridized triboelectric-electromagnetic water wave energy harvester based on a magnetic sphere. *ACS Nano*. 2019;13(2):2349-2356.
- [24] Yang H, Deng M, Tang Q, et al. A nonencapsulative pendulum-like paper-based hybrid nanogenerator for energy harvesting. *Adv Energy Mater*. 2019;9(33):1901149.
- [25] Wang ZL. Triboelectric nanogenerators as new energy technology and self-powered sensors—principles, problems and perspectives. *Faraday Discuss*. 2014;176:447-458.
- [26] Fan F-R, Tian Z-Q, Lin Wang Z. Flexible triboelectric generator. *Nano Energy*. 2012;1(2):328-334.
- [27] Wang ZL. On Maxwell's displacement current for energy and sensors: the origin of nanogenerators. *Mater Today*. 2017;20(2):74-82.
- [28] Wang ZL. Entropy theory of distributed energy for internet of things. *Nano Energy*. 2019;58:669-672.
- [29] Huang B, Wang P, Wang L, Yang S, Wu D. Recent advances in ocean wave energy harvesting by triboelectric nanogenerator: an overview. *Nanotechnol Rev*. 2020;9(1):716-735.
- [30] Wang H, Xu L, Wang Z. Advances of high-performance triboelectric nanogenerators for blue energy harvesting. *Nanoenergy Adv*. 2021;1(1):32-57.
- [31] Wang ZL, Jiang T, Xu L. Toward the blue energy dream by triboelectric nanogenerator networks. *Nano Energy*. 2017;39(39):9-23.
- [32] Zhao T, Xu M, Xiao X, Ma Y, Li Z, Wang ZL. Recent progress in blue energy harvesting for powering distributed sensors in ocean. *Nano Energy*. 2021;88:106199.
- [33] Chen H, Xing C, Li Y, Wang J, Xu Y. Triboelectric nanogenerators for a macro-scale blue energy harvesting and self-powered marine environmental monitoring system. *Sustain Energy Fuels*. 2020;4(3):1063-1077.
- [34] Li W, Wan L, Lin Y, et al. Synchronous nanogenerator with intermittent sliding friction self-excitation for water wave energy harvesting. *Nano Energy*. 2022;95:106994.
- [35] Xiao TX, Liang X, Jiang T, et al. Spherical triboelectric nanogenerators based on spring-assisted multilayered structure for efficient water wave energy harvesting. *Adv Funct Mater*. 2018;28(35):1802634.
- [36] Liu L, Yang X, Zhao L, et al. Nodding duck structure multi-track directional freestanding triboelectric nanogenerator toward low-frequency ocean wave energy harvesting. *ACS Nano*. 2021;15(6):9412-9421.
- [37] Liang X, Liu Z, Feng Y, et al. Spherical triboelectric nanogenerator based on spring-assisted swing structure for effective water wave energy harvesting. *Nano Energy*. 2021;83(83):105836.
- [38] Lin Z, Zhang B, Xie Y, Wu Z, Yang J, Wang ZL. Elastic-connection and soft-contact triboelectric nanogenerator with superior durability and efficiency. *Adv Funct Mater*. 2021;31(40):2105237.
- [39] Xu L, Xu L, Luo J, et al. Hybrid all-in-one power source based on high-performance spherical triboelectric nanogenerators for harvesting environmental energy. *Adv Energy Mater*. 2020;10(36):2001669.
- [40] Chen P, An J, Shu S, et al. Super-durable, low-wear, and high-performance fur-brush triboelectric nanogenerator for wind and water energy harvesting for smart agriculture. *Adv Energy Mater*. 2021;11(9):2003066.
- [41] Xi Y, Wang J, Zi Y, et al. High efficient harvesting of underwater ultrasonic wave energy by triboelectric nanogenerator. *Nano Energy*. 2017;38:101-108.

SUPPORTING INFORMATION

Additional supporting information can be found online in the Supporting Information section at the end of this article.

How to cite this article: Jiang Y, Chen P, Han J, et al. High-performance triboelectric nanogenerator based on a double-spiral zigzag-origami structure for continuous sensing and signal transmission in marine environment. *Interdiscip Mater*. 2025;4:201-212. doi:10.1002/idm2.12226